Characterization of Physical and Structural Properties of Brass Powder After Biofield Treatment

Mahendra Kumar Trivedi, Gopal Nayak, Shrikant Patil, Rama Mohan Tallapragada, Omprakash Latiyal, Snehasis Jana

Trivedi et al., J Powder Metall Min 2015, 4:1
http://dx.doi.org/10.4172/2168-9806.1000134

Powder Metallurgy & Mining

Research Article Open Access

Characterization of Physical and Structural Properties of Brass Powder After Biofield Treatment

Trivedi MK[2], Nayak G[2], Patil S[2], Tallapragada RM[2], Latiyal O[1] and Jana S[1]*

[1]*Trivedi Science Research Laboratory Pvt. Ltd., Hall-A, Chinar Mega Mall, Chinar Fortune City, Hoshangabad Road, Bhopal-462026, Madhya Pradesh, India*

[2]*Trivedi Global Inc., 10624 S Eastern Avenue Suite A-969, Henderson, NV 89052, USA*

Abstract

Brass, a copper-zinc (Cu-Zn) alloy has gained extensive attention in industries due to its high corrosion resistance, machinability and strength to weight ratio. The aim of present study was to evaluate the effect of biofield treatment on structural and physical properties of brass powder. The brass powder sample was divided into two parts: control and treated. The treated part was subjected to Mr.Trivedi's biofield treatment. Control and treated brass powder were characterized using particle size analyser, X-ray diffraction (XRD), scanning electron microscope (SEM), and Fourier transform infrared (FT-IR) spectroscopy. The result showed that the average particle size, d_{50} and d_{99} (size below which 99% particles were present) were reduced up to 44.3% and 56.4%, respectively as compared to control. XRD result revealed that the unit cell volume in treated brass powder was increased up to 0.19% as compared to control. Besides, the crystallite size of brass powder was significantly increased up to 100.5% as compared to control, after biofield treatment. Furthermore, SEM microscopy showed welded particles in control powder, however fractured surfaces were observed in treated sample. In FT-IR spectra, new peak at 685 cm-1 was observed after biofield treatment as compared to control that might be due to alteration in bonding properties in treated brass sample. These findings suggest that the biofield treatment has significantly altered the physical and structural properties of brass powder.

Keywords: Biofield treatment; Brass; X-ray diffraction; Fourier transform infrared; Particle size; Scanning electron microscopy

Introduction

Brass, an alloy mainly consist of copper (Cu) and zinc (Zn), is widely used in various industries because of their good formability, high corrosion resistance, strength to weight ratio, and ductility. Auto industries are always in need of light and strong automotive parts. Thus, it is possible to manufacture several parts and products for automobile applications using the brass alloy. Furthermore, high strength brass alloy contains some additional elements such as iron, manganese, tin, etc. These elements form a brittle inter metallic compound in brass, which increase the strength of the alloy but reduce the ductility and machinability [1]. During manufacturing of any parts in industries, the ductility and machinability plays a major role. On the other hand, the mechanical properties such as strength and ductility in the metal alloy are influenced by crystallite size and its distribution [2]. Currently, the crystallite size in nano material is controlled by using various heat treatment processes at certain temperature [3,4]. It is also reported that optimizing the crystallite size in material gives the desired magnetic properties [2]. Furthermore, the heat treatment processes require costly equipment set up and high power supply, to modulate the mechanical properties. Thus, after considering the properties of brass and cost aspect, authors wanted to investigate an alternative and economically safe approach that could be beneficial in global application to modify the physical and structural properties of the brass powder.

The law of mass-energy inter-conversion has existed in the literature for more than 300 years for which first idea was given by Fritz, after that Einstein derived the well-known equation $E=mc^2$ for light and mass [5,6]. However, the conversion of mass into energy is fully verified, but the inverse of this relation, i.e. energy into mass has not yet verified scientifically. Moreover, the energy exists in various forms such as kinetic, potential, electrical, magnetic, nuclear etc. which have been generated from different sources. Similarly, the human nervous system consists of neurons, which have the ability to transmit information in the form of electrical signals [7-10]. Thus, a human has the ability to harness the energy from environment/universe and can transmit into any object (living or non-living) around the Globe. The object(s) always receive the energy and responded into useful way that is called biofield energy. This process is known as biofield treatment. Mr. Trivedi's Biofield Treatment (The Trivedi Effect(R)) has been applied to transform the structural, physical and chemical properties of various metals and ceramics [11-18]. In material science, this biofield treatment has substantially decreased the particle size by 71% in zirconium oxide [17] and increased the crystallite size up to 66% in vanadium pentoxide (V_2O_5) [16]. The biofield treatment has also transformed the physical and molecular characteristics in several other fields like biotechnology [19,20], microbiology [21-23], and agriculture [24-26].

Based on the outstanding results achieved by biofield treatment on different materials and considering the industrial significance of brass powder, the present study was undertaken to evaluate the impact of biofield treatment on physical and structural properties of brass powder.

Experimental

Brass powder was procured from Alfa Aesar, USA. The brass powder sample was equally distributed into two parts, one part was considered as control and another part was subjected to Mr. Trivedi's

***Corresponding author:** Jana S, Trivedi Science Research Laboratory Pvt. Ltd., Hall-A, Chinar Mega Mall, Chinar Fortune City, Hoshangabad Road, Bhopal-462026, Madhya Pradesh, India, Tel: +91-755-6660006; E-mail: publication@trivedisrl.com

Received June 29, 2015; **Accepted** July 14, 2015; **Published** July 27, 2015

Citation: Trivedi MK, Nayak G, Patil S, Tallapragada RM, Latiyal O, et al. (2015) Characterization of Physical and Structural Properties of Brass Powder After Biofield Treatment. J Powder Metall Min 4: 134. doi:10.4172/2168-9806.1000134

biofield treatment, referred as treated. The control and treated samples were characterized by using particle size analyzer, X-ray diffraction (XRD), scanning electron microscopy (SEM), and Fourier transform infrared (FT-IR) spectroscopy.

Particle size analysis

For particle size analysis, Laser particle size analyzer SYMPATEC HELOS-BF was used with a detection range of 0·1-875 µm. The particle size data was collected in the chart form of particle size vs. cumulative percentage. Average particle size, d_{50} and d_{99} (size below which 99%, particles are present) were calculated from the particle size distribution curve. The percent changes in particle size were calculated using following equations:

$$\%change\,in\,particle\,size, d_{50} = \frac{\left[(d_{50})_{Treated} - (d_{50})_{Control}\right]}{(d_{50})_{Control}} \times 100$$

Where, $(d_{50})_{Control}$ and $(d_{50})_{Treated}$ are the particle size, d_{50} of control and treated samples respectively.

$$\%change\,in\,particle\,size, d_{99} = \frac{\left[(d_{99})_{Treated} - (d_{99})_{Control}\right]}{(d_{99})_{Control}} \times 100$$

Where, $(d_{99})_{Control}$ and $(d_{99})_{Treated}$ are the particle size, d_{99} of control and treated samples.

For particle size evaluation, treated part was further divided into four equal parts, referred as T1, T2, T3, and T4.

X-ray diffraction study

XRD analysis was carried out on Phillips, Holland PW 1710 X-ray diffractometer system, which had a copper anode with nickel filter. The radiation of wavelength used by this XRD system was 1.54056 Å. The data obtained from this XRD were in the form of a chart of 2θ *vs.* intensity and a detailed table containing peak intensity counts, d value (Å), peak width (θ°), relative intensity (%) etc. Additionally, Powder X software was used to calculate lattice parameter and unit cell volume.

The crystallite size (L) was calculated by using formula:

$L = k\lambda/(b\cos\theta)$,

Here, λ is the wavelength of radiation used and k is the equipment constant (=0.94), b is full width half maximum of peak (FWHM). The percentage change in all parameters such as lattice parameter, unit cell volume and crystallite size were calculated using the following equations:

Percent change in lattice parameter=$[(a_t-a_c)/a_c] \times 100$

Where, a_c and a_t are lattice parameter value of control and treated powder samples respectively

Percent change in unit cell volume=$[(V_t-V_c)/V_c] \times 100$

Where, V_c and V_t are the unit cell volume of control and treated powder samples respectively

Percent change in crystallite size=$[(L_t-L_c)/L_c] \times 100$

Where, L_c and L_t are crystallite size of control and treated powder samples respectively. XRD analysis was carried out for control and treated T1, T2, T3 and T4 brass samples.

Scanning electron microscopy (SEM)

Structure and surface morphology are the unique properties of brass powder. Control and treated brass was observed using JEOL JSM-6360 SEM instrument at 2000x magnification. Differences in the tendency of the particles to clump were easily seen at the lower magnifications, while variations in size and morphology become clearer at higher magnification [27].

FT-IR spectroscopy

FT-IR analysis of control and treated samples were performed on Shimadzu, Fourier Transform Infrared (FT-IR) Spectrometer with frequency range of 4000-300 cm^{-1}.

Results and Discussion

Particle size analysis

The particle size of control and treated brass powder are presented in Figures 1 and 2. It showed that the average particle size (d_{50}) was 40 µm in control, whereas 22.9, 24.1, 22.3, and 37 µm in treated T1, T2, T3, and T4 respectively (Figure 1). This indicates that the d_{50} was significantly reduced by 42.8, 39.8, 44.3, and 7.5% in T1, T2, T3, and T4 brass samples respectively, as compared to control. In addition, the particle size, d_{99} was 180.9, 90, 78.9, 88.3, 115.8 µm in control, T1, T2, T3 and T4 respectively. This indicates that d_{99} was substantially reduced by 50.2, 56.4, 51.2, and 36% in T1, T2, T3 and T4 respectively, as compared to control (Figure 2). Overall, particle size analysis result revealed that the sizes of particles were reduced in all treated brass samples as compared to control. Furthermore, the significant reduction of particle size found in d_{50} and d_{99} suggest that percent of coarser particles in brass powder were reduced after biofield treatment.

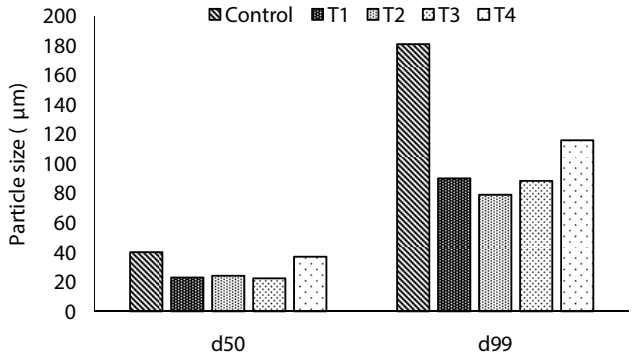

Figure 1: Effect of biofield treatment on particle size of brass powder.

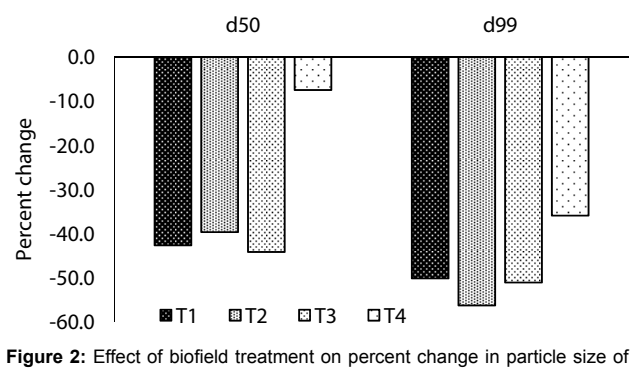

Figure 2: Effect of biofield treatment on percent change in particle size of brass powder.

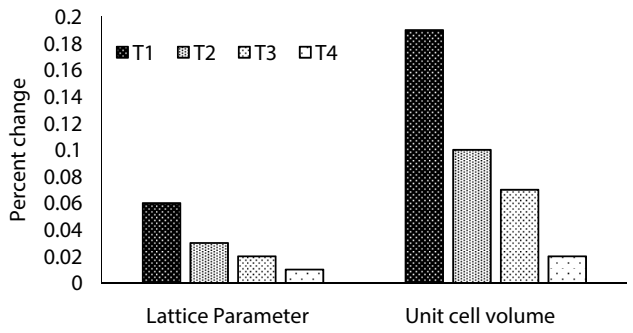

Figure 3: Effect of biofield treatment on lattice parameter and unit cell volume of brass powder.

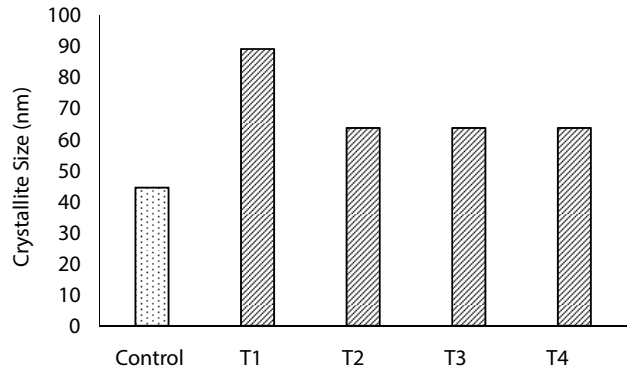

Figure 4: Effect of biofield treatment on crystallite size of brass powder.

This could be possible if coarser particles were fractured into smaller particles after treatment. Hence, it is hypothesised that energy might be transferred to powder during biofield treatment, which probably induced the energy milling in brass powder. This energy milling in brass may lead to fracture the coarse particles and reduced particle size [13,14]. Further, in order to understand the effect of biofield treatment at structural and atomic level, XRD was carried out for control and treated samples of brass.

X-ray diffraction study

XRD analysis result of control and treated brass are illustrated in Figures 3-5. It was observed that lattice parameter and unit cell volume increased up to 0.06% and 0.19%, respectively as compared to control (Figure 3). Furthermore, it is well known that stress and volumetric strain have direct relationship as per Hooke's law, which is given as follow [28]:

$$\sigma = K \varepsilon \quad (1)$$

Where, σ is stress applied, K is bulk modulus, and ε is volumetric strain

Moreover, in this experiment, the treated sample showed volumetric strain (up to 0.19%) as compared to control, which indicates that a stress may have been applied through biofield treatment as per equation (1). Besides this, the crystallite size was increased from 44.4 nm (control) to 89 nm, 63.6 nm, 63.6 nm, and 63.6 nm in treated T1, T2, T3, and T4 respectively (Figure 4). This suggests that crystallite size of treated brass sample was significantly increased up to 100.5% (T1) as compared to control (Figure 5). This increase in crystallite size in treated brass powder may be due to re-orientation of neighbouring plane into same plane after biofield treatment. On the other hand, it is reported that a material with a large crystallite size shows more ductility than powder with fine nanostructures [29]. Thus, it is postulated that biofield treated brass powder with higher crystallite size might have higher ductility than control.

SEM analysis

On the basis of particle size result, the reduction was found

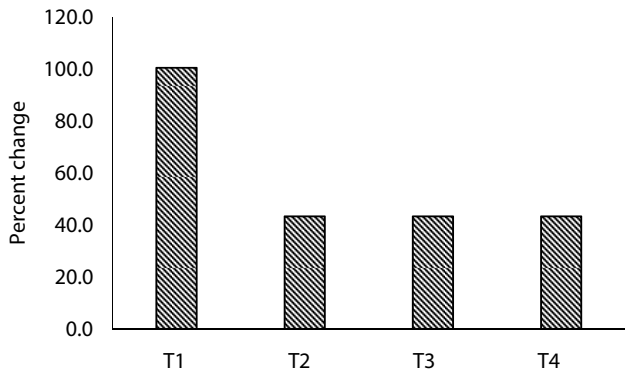

Figure 5: Effect of biofield treatment on percent change in crystallite size of brass.

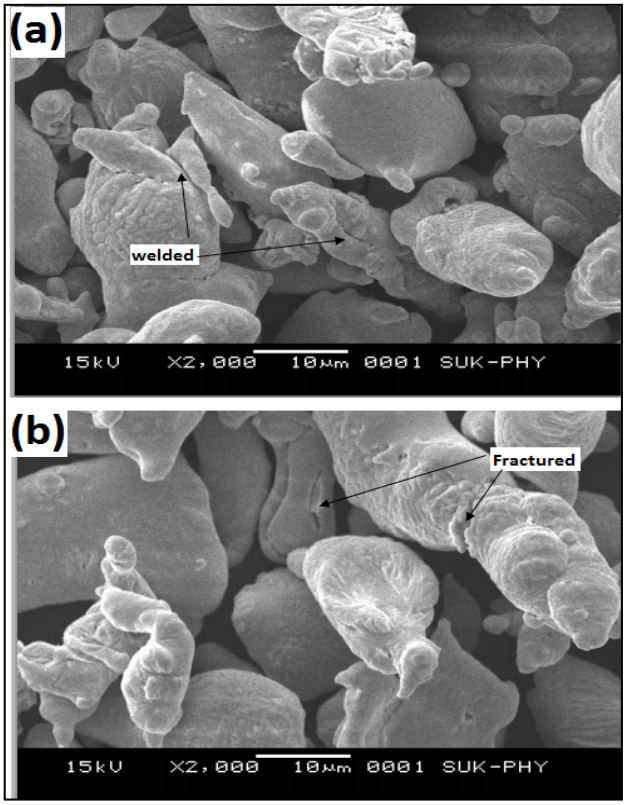

Figure 6: The SEM image of (a) control and (b) treated brass powder (T1).

maximum in T1 as compared to other groups, thus it was further analysed microscopically using SEM. Surface morphology of control and treated brass powder are shown in Figure 6. Control brass sample shows the atomized, tear drop shaped welded particles, whereas fractured at satellites and intra particle boundaries were observed in treated brass sample. It indicates that brass powder particles were fractured after biofield treatment. Similar kind of surface morphology was also observed in biofield treated lead powder [15]. Thus, it is speculated that the biofield treatment may induced stress energy that resulted into high energy milling. Further, this high energy milling probably induced fractures in the particles.

FT-IR spectroscopy

The FT-IR spectrum of control and treated sample (T1) of brass are presented in Figure 7. In IR spectra, the band observed at wave number 3450 cm^{-1} (control) and 3439 cm^{-1} (treated) were assigned to O-H stretching due to water absorption by samples. Band at wave number 1652 cm^{-1} (control) and 1637 cm^{-1} (treated) were attributed to H-O-H bending vibration [30]. The absorption peak at wave number 792 cm^{-1} observed in control and treated sample was attributed to Zn–O–H and Cu-O-H vibrations. In addition, a new peak was found at wave number 685 cm^{-1} in IR spectra of treated brass as compared to control that might be due to Cu_2O vibrations [31]. It is hypothesised that biofield energy may be acting at atomic level to cause this modification.

Conclusion

Herein, study reports the influence of biofield treatment on brass powders at its structural and physical properties. A significant decrease in particles size up to 44.3% was found in treated brass as compared to control that may be due to fracturing of powder particles through high energy milling induced by biofield treatment. In addition, XRD data revealed that the biofield has substantially increased the crystallite size in treated brass powder up to 100.5% as compared to control. This increase in crystallite size in treated brass powder may result into higher ductility and machinability. Thus, it is postulated that biofield treatment could be applied to improve the mechanical properties of brass powder for automobile and transport equipment applications.

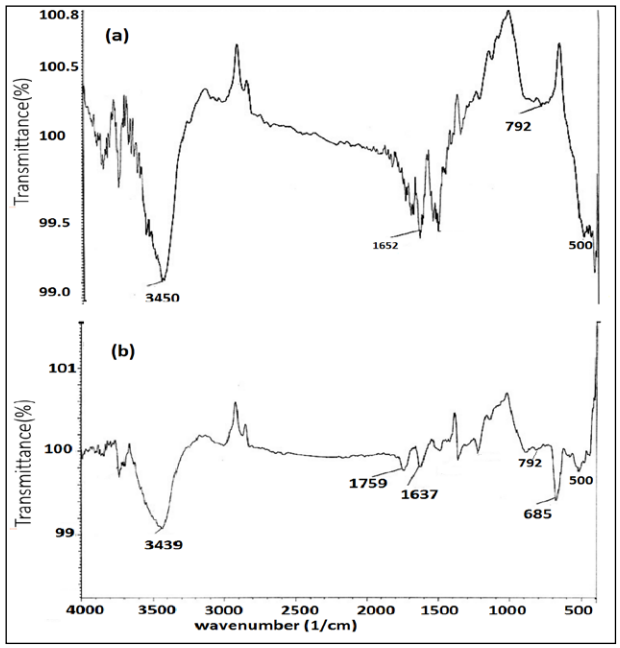

Figure 7: FT-IR spectrum of (a) Control and (b) Treated brass powder (T1).

Acknowledgement

We thank Dr. Cheng Dong of NLSC, Institute of Physics, and Chinese academy of Sciences for their support in using Powder X software for analyzing X-ray Diffraction results.

References

1. Imai H, Li S, Kondoh K, Kosaka Y, Okada T, et al. (2014) Microstructure and mechanical properties of Cu-40 percent Zn-0.5 percent Cr alloy by powder metallurgy. Mater Trans 55: 528-533.
2. Anderson JC (2004) Materials science for engineers. CRC Press, London.
3. Mohammadzadeh A, Namini AS, Azadbeh M (2014) Densification and microstructure characteristics of a pre alloyed alpha brass powder processed by liquid phase sintering. Iranian J Material Sci and Eng 11: 67-74.
4. Shufeng L, Hisashi I, Haruhiko A, Katsuyoshi K (2011) Fabrication of high-strength Cu40ZnSnTi brass via powder metallurgy and hot extrusion. Trans JWRI 40: 59-62.
5. Hasenohrl F (1904) On the theory of radiation in moving bodies. Annalen der Physik 15: 344-370.
6. Einstein A (1905) Does the inertia of a body depend upon its energy-content. Annalen der Physik 18: 639-641.
7. Becker RO, Selden G (1985) The body electric: Electromagnetism and the foundation of life, William Morrow and Company, New York City.
8. Barnes RB (1963) Thermography of the human body. Science 140: 870-877.
9. Born M (1971) The Born-Einstein Letters. Walker and Company, New York.
10. Cohen S, Popp FA (2003) Biophoton emission of the human body. Indian J Exp Biol 41: 440-445.
11. Trivedi MK, Tallapragada RM (2008) A transcendental to changing metal powder characteristics. Met Powder Rep 63: 22-28, 31.
12. Trivedi MK, Tallapragada RM (2009) Effect of super consciousness external energy on atomic, crystalline and powder characteristics of carbon allotrope powders. Mater Res Innov 13: 473-480.
13. Dhabade VV, Tallapragada RM, Trivedi MK (2009) Effect of external energy on atomic, crystalline and powder characteristics of antimony and bismuth powders. Bull Mater Sci 32: 471-479.
14. Trivedi MK, Patil S, Tallapragada RM (2012) Thought Intervention through bio field changing metal powder characteristics experiments on powder characteristics at a PM plant. Proceeding of the 2nd International Conference on Future Control and Automation 2: 247-252.
15. Trivedi MK, Patil S, Tallapragada RM (2013) Effect of biofield treatment on the physical and thermal characteristics of silicon, tin and lead powders. J Material Sci Eng 2: 125-132.
16. Trivedi MK, Patil S, Tallapragada RM (2013) Effect of biofield treatment on the physical and thermal characteristics of vanadium pentoxide powder. J Material Sci Eng S11: 001.
17. Trivedi MK, Patil S, Tallapragada RM (2014) Atomic, crystalline and powder characteristics of treated zirconia and silica powders. J Material Sci Eng 3: 144.
18. Trivedi MK, Patil S, Tallapragada RM (2015) Effect of biofield treatment on the physical and thermal characteristics of aluminium powders. Ind Eng Manage 4: 151.
19. Patil S, Nayak GB, Barve SS, Tembe RP, Khan RR (2012) Impact of biofield treatment on growth and anatomical characteristics of *Pogostemon cablin* (Benth.). Biotechnology 11: 154-162.
20. Altekar N, Nayak G (2015) Effect of biofield treatment on plant growth and adaptation. J Environ Health Sci 1: 1-9.
21. Trivedi MK, Patil S, Bhardwaj Y (2008) Impact of an external energy on *Staphylococcus epidermis* [ATCC –13518] in relation to antibiotic susceptibility and biochemical reactions- An experimental study. J Accord Integr Med 4: 230-235.
22. Trivedi MK, Patil S (2008) Impact of an external energy on *Yersinia enterocolitica* [ATCC –23715] in relation to antibiotic susceptibility and biochemical reactions: An experimental study. Internet J Alternat Med 6: 13.

23. Trivedi MK, Patil S, Bhardwaj Y (2009) Impact of an external energy on *Enterococcus faecalis* [ATCC – 51299] in relation to antibiotic susceptibility and biochemical reactions - An experimental study. J Accord Integr Med 5: 119-130.

24. Shinde V, Sances F, Patil S, Spence A (2012) Impact of biofield treatment on growth and yield of lettuce and tomato. Aust J Basic Appl Sci 6: 100-105.

25. Lenssen AW (2013) Biofield and fungicide seed treatment influences on soybean productivity, seed quality and weed community. Agricultural Journal 8: 138-143.

26. Sances F, Flora E, Patil S, Spence A, Shinde V (2013) Impact of biofield treatment on ginseng and organic blueberry yield. Agrivita J Agric Sci.

27. Dercz G, Prusik K, Pająk L (2008) X-ray and SEM studies on zirconia powders. JMME 31: 408-414.

28. Ugural AC (2011) Advanced strength and applied elasticity. Pearson Education.

29. Kairet T, Degrez M, Campana F, Janssen JP (2007) Influence of the powder size distribution on the microstructure of cold-sprayed copper coating studies by X-ray diffraction. J Therm Spray Technol 16: 610-618.

30. Ravichandran R, Nanjundan S, Rajendran N (2004) Effect of benzotriazole derivatives on the corrosion of brass in NaCl solutions. Appl Surf Sci 236: 241-250.

31. Zhang X, Wallinder IO, Leygraf C (2014) Mechanistic studies of corrosion product flaking on copper and copper-based alloys in marine environments. Corr Sci 85: 15-25.

Citation: Trivedi MK, Nayak G, Patil S, Tallapragada RM, Latiyal O, et al. (2015) Characterization of Physical and Structural Properties of Brass Powder After Biofield Treatment. J Powder Metall Min 4: 134. doi:10.4172/2168-9806.1000134